

Impact of the Carbene Derivative Charge on the Decomposition Rates of Hoveyda–Grubbs-like Metathesis Catalysts

Magdalena Jawiczuk,[§] Anna Marczyk,[§] Katarzyna Młodzikowska-Pieńko,[§] and Bartosz Trzaskowski*

Cite This: *J. Phys. Chem. A* 2020, 124, 6158–6167

Read Online

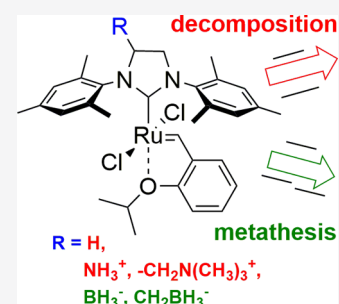
ACCESS |

Metrics & More

Article Recommendations

Supporting Information

ABSTRACT: Hoveyda–Grubbs metathesis catalysts undergo a relatively fast decomposition in the presence of olefins. Using a computational density functional theory approach, we show that positively charged derivatives of N-heterocyclic carbenes have little impact on the degradation/deactivation rates of such catalysts with respect to neutral carbenes. On the other hand, the hypothetical anionic Hoveyda–Grubbs-like catalysts are predicted to less likely undergo degradation in the presence of the olefin, while being as active as standard, neutral Hoveyda–Grubbs catalysts.



1. INTRODUCTION

The phenomenon of N-heterocyclic carbenes (NHCs) started in 1991, when they were first synthesized by Arduengo.¹ Since then, these ligands have been widely used in various aspects of chemical synthesis, mostly in organometallic chemistry.² NHCs have the ability to coordinate a large number of elements, including transition metals, which makes them useful both in homogenous and heterogenous catalysis.³ One of the most popular applications of NHCs is as ruthenium olefin metathesis catalysts and, in particular, the Hoveyda–Grubbs complex.⁴ Since the discovery of these ruthenium complexes in 1999, a lot of research has been devoted to better understanding of chemical and electronic properties of NHCs and their effect on ruthenium metathesis complexes.^{5,6}

One of the recently suggested and introduced modifications of carbenes is the addition of a positive or negative charge to NHCs. Anionic NHCs (Figure 1a) were obtained both in the isolated form and in metal complexes,^{7–16} and in the latter systems, they were shown to possess, in general, good stability because of their high affinity for transition metals bearing a formal positive charge.¹⁷ Surprisingly, however, there is not a single example of any of the anionic NHC derivatives complexing Ru to form a potential metathesis catalyst, although such systems have been proposed in computational studies and predicted to be stable and good candidates for efficient metathesis catalysts.^{18,19} The cationic NHCs (Figure 1b) were also reported,^{20–26} and it was shown that the positive charge on the NHC affects the electron properties by reducing the σ -donation properties and slightly increasing the π -acidity. Despite their weak electron-donor properties, multiple complexes with transition metals for cationic carbenes were also obtained.²⁷ In the context of olefin metathesis, cationic carbenes are commonly used for more than 10 years to obtain

water-soluble catalysts by introducing various ammonium-tagged moieties.^{26,28–30} Interestingly, it has been shown both experimentally and theoretically that the impact of the additional positive charge on the reactivity of such systems is very low.^{31,32}

Modification of NHCs' structure and charge may affect the electronic properties of complexes with transition metals, which results in changes in their organometallic applications,^{33,34} but also, it is likely to affect the decomposition rates and pathways of such systems. Decomposition studies of ruthenium complexes were first reported by Grubbs et al. where he investigated Grubbs-type catalysts (both first and second generation) and observed a significant effect of the used solvent on the formation of intermediates.¹⁵ They also confirmed the presence of a dinuclear ruthenium compound and its influence on reaction side effects such as olefin isomerization.³⁵ Further research led to the conclusion that the phosphine fragment is also involved in the decomposition process.³⁶ Two years later, van Rensburg suggested a substrate-induced decomposition mechanism for both Grubbs and Hoveyda–Grubbs catalysts involving a beta-hydride transfer from the ruthenacyclobutane intermediate.³⁷ This mechanism is believed to be the major olefin-dependent decomposition path.^{38,39} The proposed mechanism of decomposition (Figure 2) consists of several stages: dissociation of the phosphine or carbene (steps 1 and 2), coordination of the ethylene to the

Received: April 7, 2020

Revised: July 3, 2020

Published: July 8, 2020



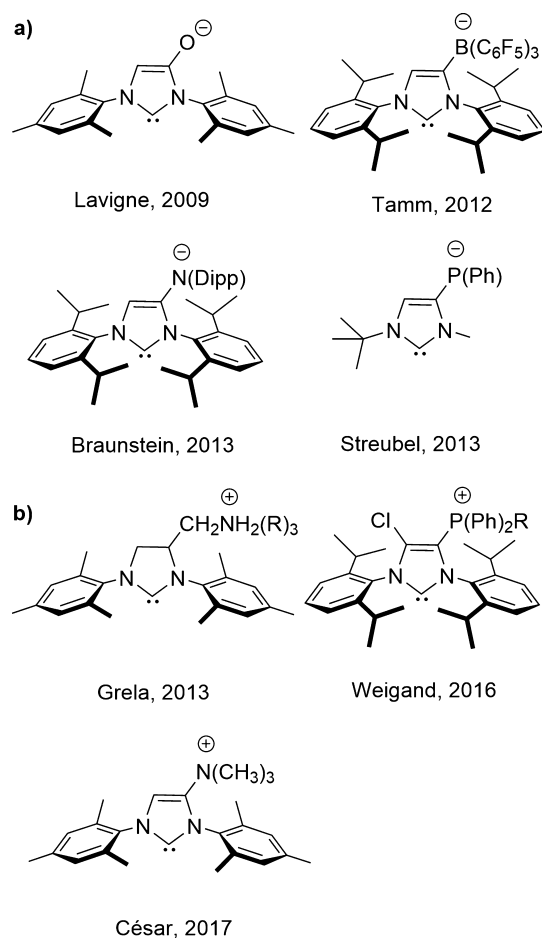


Figure 1. Selected examples of (a) anionic and (b) cationic ligands.

unsaturated 14 electron complex (step 3), beta-hydride transfer in the ruthenacyclobutane precursor (step 4), formation of a Ru(IV) allyl-hydride species (step 5), and reductive transfer of the hydride to the terminal position of the allylic fragment (step 6). These steps result in the formation of an unsaturated Ru(II) complex, which is inactive in metathesis reaction.³⁷ Two other olefin-driven decomposition mechanisms have been proposed recently by Jensen and Fogg. Jensen showed that olefins bearing at least three carbon atoms may decompose ruthenium catalysts using a mechanism different from the van Rensburg one with a computationally estimated barrier of 29.5 kcal/mol.⁴⁰ Later, Fogg showed that bimolecular methylidene coupling is also a viable decomposition pathway for metathesis catalysts.^{38,39} Other known decomposition routes which may involve Buchner-type ring expansion reaction or alcohol/amine-driven degradation may occur only in the presence of external agents and are outside the scope of this investigation.^{41–50}

There are many known examples of structural modification in neutral carbenes, which alter the stabilities of Hoveyda–

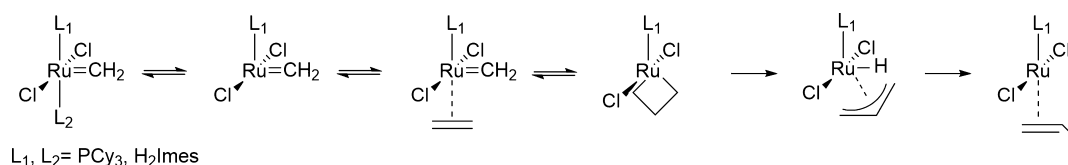


Figure 2. Decomposition mechanism reported by van Rensburg.

Grubbs-like catalysts.^{25,30} On the other hand, the possible impact of the introduction of extra charge into carbene on the decomposition of Hoveyda–Grubbs-like catalysts has not yet been studied. In this work, we used density functional theory (DFT) calculations to compare the decomposition of the Hoveyda–Grubbs catalyst and its derivatives bearing selected, model anionic and cationic NHC moieties (Figure 3). Because

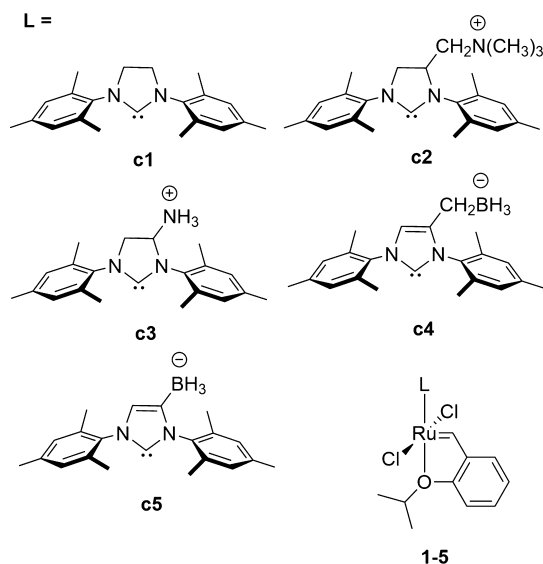


Figure 3. Neutral, cationic, and anionic Hoveyda–Grubbs model carbenes studied in this work.

of different charge distributions in investigated complexes, we focused on their electronic properties and energetics of the entire decomposition pathway and show structure–decomposition rate relationships for this important family of catalysts. For this task, we selected two important olefins: ethylene and more bulky allylbenzene, which were previously used in computational studies of olefin metathesis.⁴⁰ The model carbenes we used were built based on known, similar catalysts (for cationic systems) or known, similar carbenes (for anionic systems).^{13,51}

2. COMPUTATIONAL METHODS

In this study, we used a computational approach similar to our previous studies on ruthenium metathesis catalysts and carbenes, validated against experimental data.^{18,32,33,49,52–56} In short, all starting models of all stationary points and transition states for all systems were prepared on the basis of the crystal structure of precatalyst **1**.⁵⁷ For monomers, Gibbs free energies used throughout the text are the sum of electronic energy (M06/LACV3P++**//B3LYP/LACVP**), solvation energy (single-point Poisson–Boltzmann self-consistent polarizable continuum method in toluene), zero-point energy correction, thermal correction to enthalpy, and the negative

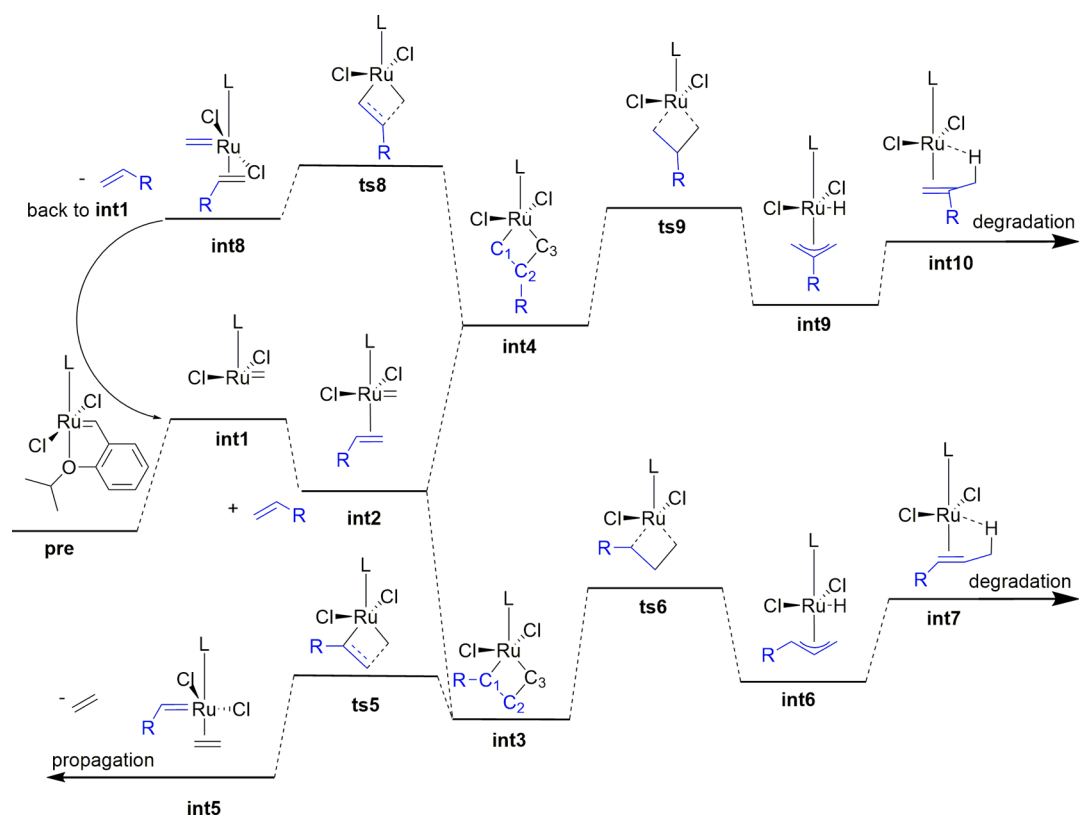


Figure 4. Initiation and first part of the propagation phase in the metathesis catalytic cycle with possible degradation pathways in this part of the catalytic cycle and the atom numbering scheme used throughout this work.

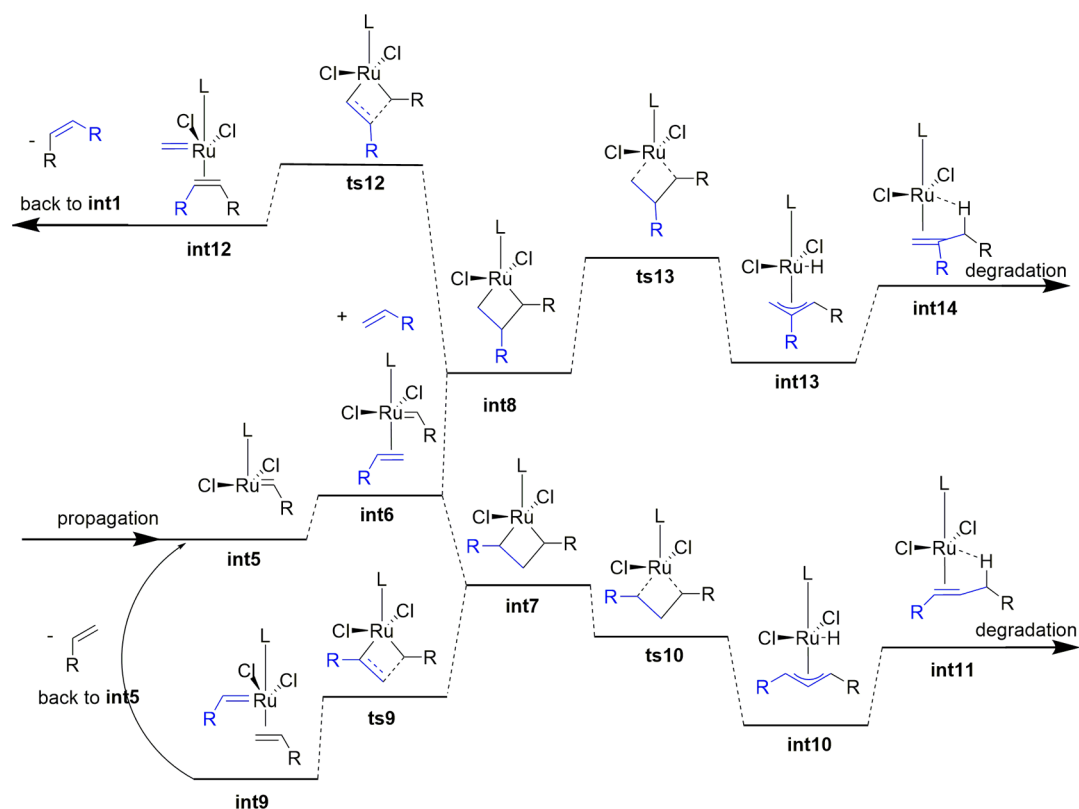


Figure 5. Second part of the propagation phase of the metathesis catalytic cycle and possible degradation pathways.

product of temperature and entropy, all at 298 K. In the case of Ru dimers, both the B3LYP and M06 optimizations in the

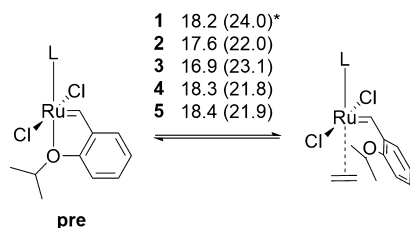
LACVP** basis set yielded dimers with a very long Ru–Ru distance (above 3.0 Å); therefore, we optimized them using the

ERMLER2 ECP basis set with the B3LYP-D3 functional.⁵⁸ All other calculations of Gibbs free energies for dimers were performed as mentioned above with single-point M06/LACV3P++** electronic energies. We used standard convergence criteria and fine grid for DFT calculations, as implemented in Jaguar ver. 9.5.⁵⁹ The relative Gibbs free energy of all systems was calculated with respect to the complex consisting of the precatalyst of each system interacting with the ethylene molecule, but with the solvation energy calculated separately for the precatalyst and ethylene. For each structure, frequencies were calculated to verify the nature of each stationary point (zero imaginary frequencies for minima and one for transition states). For intermediates **1_int7 B** and **2_int_dim**, we were not able to obtain a converged system with zero imaginary frequencies and instead used a geometry with one very small (below $i3\text{ cm}^{-1}$ for **1_int7 B** and below $i14\text{ cm}^{-1}$ for **2_int_dim**) imaginary frequency. Gibbs free energy barriers for the bimolecular coupling decomposition pathway were estimated as the sum of Gibbs free energies of the corresponding intermediates and energy evaluations based on the maximum-energy structures of the potential energy surface scans performed for the C–C methyldene carbon atoms.

3. RESULTS AND DISCUSSION

The general scheme of the metathesis catalytic cycle combined with decomposition pathways with olefin is presented in Figures 4 and 5 together with the atom naming scheme used throughout this study.

Before exploring the decomposition pathways, we shortly explored the olefin metathesis using these charged complexes. Earlier, Ashworth and Plenio have shown that the Hoveyda–Grubbs catalyst initiates using, preferably, an interchange mechanism for small olefins and via a dissociative mechanism for larger ones and the precatalyst activation step is the rate-limiting step for the entire catalytic cycle.^{60,61} Olefin studies, in this work, are also small, but, nevertheless, we decided to perform calculations for both the interchange and dissociative mechanisms. As expected, in all cases, the interchange transition state has a lower barrier than the dissociation one and rather similar to **1** (see Figure 6). As a result, we can



1	18.2 (24.0)*
2	17.6 (22.0)
3	16.9 (23.1)
4	18.3 (21.8)
5	18.4 (21.9)

Figure 6. Gibbs free energies for the activation of precatalysts **1–5** with ethylene using interchange mechanisms. Numbers in parentheses correspond to Gibbs free energies for the dissociative mechanism. The values for **1** are taken from ref 50.

expect that the initiation phase with all studied complexes takes place similarly to the Hoveyda–Grubbs catalyst, and metallacyclobutane intermediates **int3/int4**, crucial for decomposition, are produced.

The olefin metathesis/degradation pathways for the Hoveyda–Grubbs catalysts in the presence of ethylene and allylbenzene, two model olefins widely used in numerous experimental and computational studies, are presented in Figure 7. The results using our computational approach are

very similar to the computational results presented earlier.⁶² The crucial Gibbs free energy barrier of the transition state between metallacyclobutane (**int3**) and ruthenium hydride (**ts6**) is estimated as 26.8 kcal/mol for ethylene and catalyst **1**, in agreement with the estimates for the degradation barrier of the second generation Grubbs complex of van Rensburg (23.4 kcal/mol) and Jensen (24.8 kcal/mol).^{37,40} In the case of the allylbenzene-driven degradation, our free energy barrier estimate is 24.0 kcal/mol. The difference in barriers between metathesis (**ts5**) and decomposition (**ts6**) is estimated as 17.7 kcal/mol for ethylene and 20.7 kcal/mol for allylbenzene (Figure 6), also in agreement with former computational data.⁶⁰ It is worth mentioning that for **1**, as well as all other catalysts, the **int4** intermediate always has substantially higher Gibbs free energy than **int3** (in all cases, in the 2–5 kcal/mol range, see the Supporting Information); therefore, decomposition via the **ts9** transition state is not likely from the energetic point of view.

The introduction of the additional positive charge to carbene has a relatively small effect on the entire degradation pathway, and the critical energy barriers for both **2** and **3** remain similar to the Hoveyda–Grubbs case (Figure 8). The relative Gibbs free energies of all intermediates of **2/3** with respect to the precatalyst are somewhat higher than those for the neutral catalysts, which suggests slightly lower thermodynamic stability, particularly for the short-lived methyldene species (**int1**). The formation of metallacyclobutane, however, is predicted to proceed as efficiently as in the Hoveyda–Grubbs case. In the next step, after the metallacyclobutane species (**int3/int4**) formation, there are two possible pathways which the catalyst can follow, the degradation (**ts6**) or the propagation of the catalytic cycle (**ts5**). Gibbs free energy barriers for **2/3** degradation are equal to 25–29 kcal/mol, which is slightly higher than those of the Hoveyda–Grubbs catalyst, suggesting, at the first sight, a somewhat lower propensity of degradation. The comparison with the Gibbs free energy barrier for catalytic cycle propagation (**ts5**) reveals, however, that the differences between the barriers of **ts6** and **ts5** are in the 16–20 kcal/mol range, which is almost identical to the 18–21 kcal/mol range of the Hoveyda–Grubbs catalyst. Clearly, the addition of the formal positive charge has little impact on the energetic features of the catalytic cycle, even for systems with the $-\text{NH}_3^+$ group attached directly to carbene. These results are consistent with our former calculations and experimental results, indicating that the introduction of ammonium tags at different distances from the carbene core has limited influence on the catalytic properties of ruthenium metathesis catalysts bearing such carbenes.^{31,32,51}

Carbene derivatives bearing a formal -1 charge (**4/5**) have a different and quite interesting impact on both the catalytic cycle and the degradation rates of Hoveyda–Grubbs-like catalysts. First, their relative Gibbs free energies are relatively low with respect to the precatalyst, suggesting higher intrinsic stability (Figure 9). The energy barrier for the decomposition's crucial transition state (**ts6**) is equal to 22–24 kcal/mol, similar to the Hoveyda–Grubbs catalyst. However, as the metallacyclobutane intermediates **int3/int4** have lower energies with respect to the precatalyst than **1**, the differences between the degradation (**ts6**) and propagation (**ts5**) transition states are larger than those for **1** with the exception of **5** and the route with ethylene. These results suggest much lower propensity of this catalyst to undergo degradation. Clearly, the addition of the formal -1 charge alters the

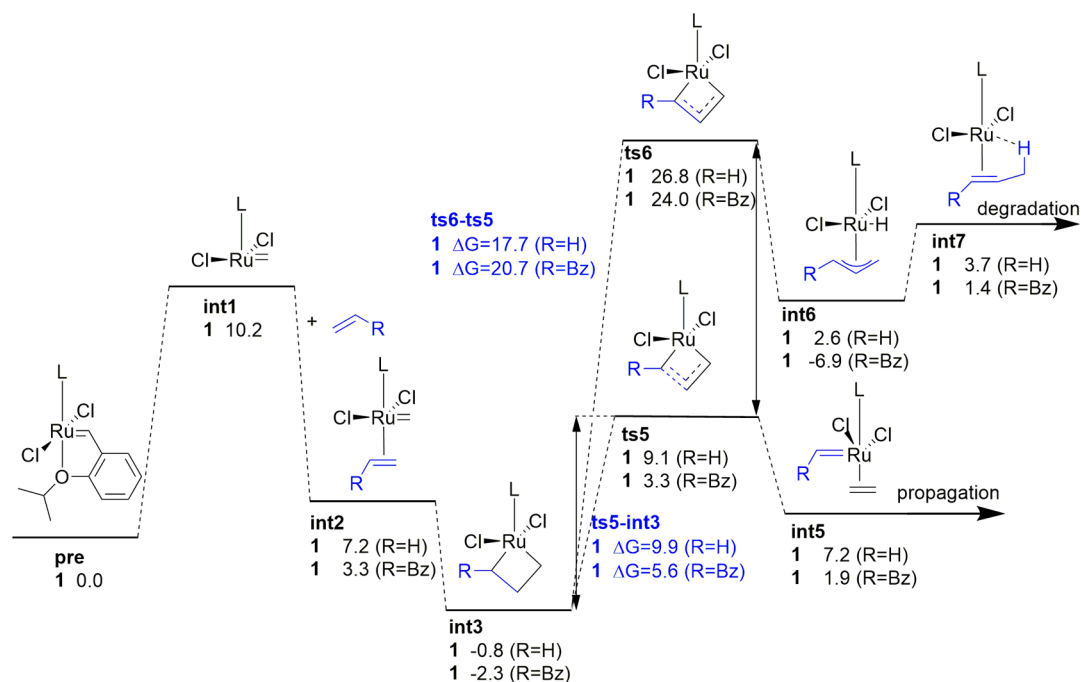


Figure 7. Relative Gibbs free energies profile (kcal/mol) of the catalytic initiation cycle/catalyst degradation for Hoveyda–Grubbs catalyst 1.

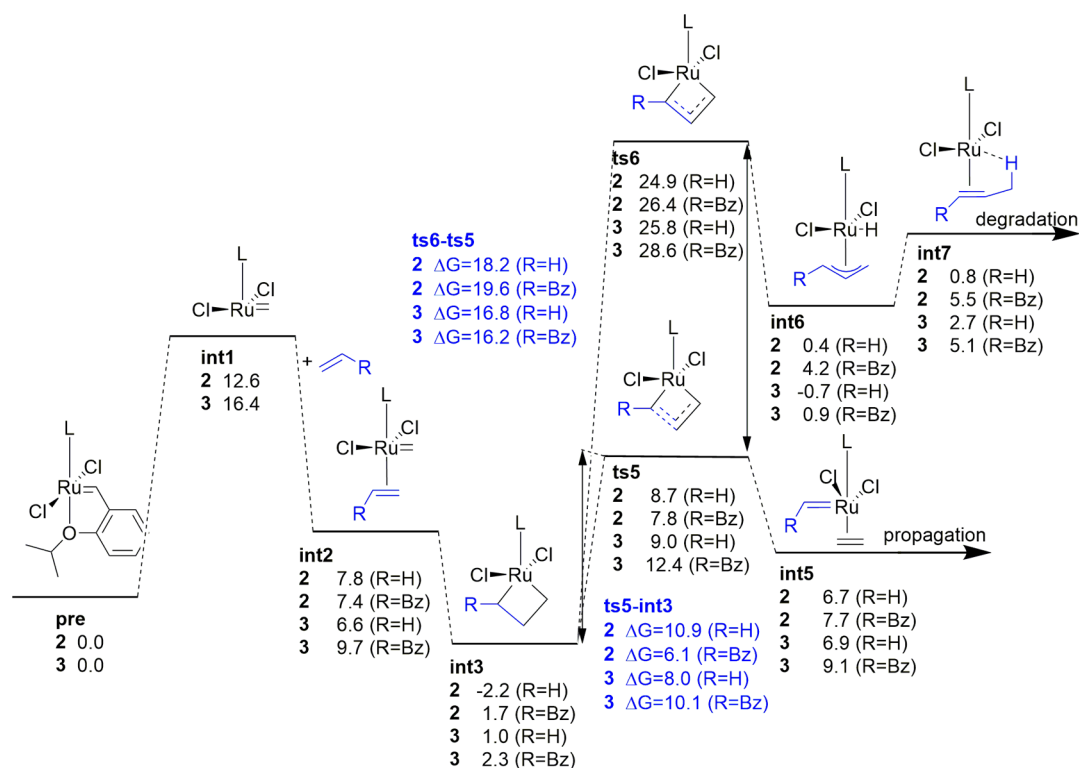


Figure 8. Relative Gibbs free energies profile (kcal/mol) of the catalytic initiation cycle/catalyst degradation for catalyst 2/3.

electronic/geometric properties of negatively charged derivatives in such a manner that the propagation pathway becomes more likely with respect to the decomposition route. This is accomplished by lowering Gibbs free energies of both the degradation and propagation transition states with respect to the neutral catalyst 1, but to a different extent.

To better understand the differences in energetic features between the investigated complexes, we decided to perform a thorough structural analysis of each of the stationary points.

Interestingly, the geometric features of 4/5 in all steps of the catalytic cycle and degradation pathway are rather similar to both the Hoveyda–Grubbs catalysts and the cationic derivatives 2/3, with only small differences in the Ru–C1 and Ru–C3 bond lengths and only in the geometries of the transition states (see Table 1 and Supporting Information). More differences can be found in the partial charges of various intermediates and transition states of the catalytic cycle, although mostly for the anionic derivative. In all cases, the

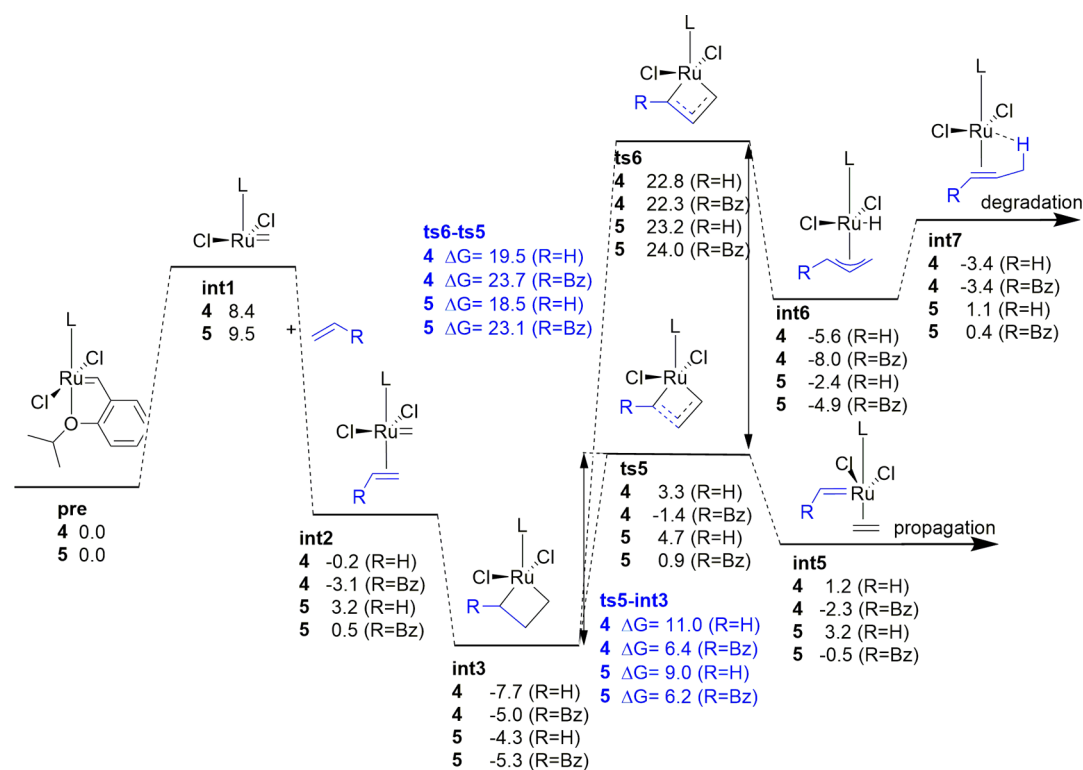


Figure 9. Relative Gibbs free energy profile (kcal/mol) of the catalytic initiation cycle/catalyst degradation for catalyst 4/5.

Table 1. Selected Geometrical Parameters (in Å) and Mulliken Partial Charges (in e) of Complexes 1, 3, and 5 in Various Stages of the Catalytic Cycle/Degradation Pathways with Ethylene as Olefin

system	Ru-C _{carbene}	Ru-O	Ru-C1	Ru-C2	Ru-C3	C1-C2	C2-C3	Ru	O	C _{carbene}	C1	C2	C3
1 pre	2.01	2.37						0.05	-0.16	0.31			
1 int1	1.94							-0.01		0.32			-0.34
1 int2	2.05		2.36	2.52		1.37		-0.07		0.26	-0.28	-0.16	-0.28
1 int3	2.05		1.98	2.28	1.98	1.59	1.59	0.08		0.22	-0.33	-0.26	-0.33
1 ts5	2.07		2.21	2.41	1.84	1.40	2.27	0.05		0.23	-0.28	-0.20	-0.35
1 ts6	2.16		2.10	2.16	2.21	1.47	1.46	0.01		0.14	-0.21	-0.31	-0.22
3 pre	1.95	2.34						0.04	-0.21	0.28			
3 int1	1.93							0.04		0.29			-0.35
3 int2	2.00		2.36	2.53		1.37		-0.05		0.22	-0.29	-0.17	-0.30
3 int3	2.01		1.98	2.28	1.98	1.58	1.59	0.15		0.18	-0.33	-0.30	-0.33
3 ts5	2.02		2.21	2.41		1.40	2.24	0.05		0.19	-0.28	-0.23	-0.36
3 ts6	2.11		2.29	2.18	2.11	1.43	1.47	-0.04		0.16	-0.21	-0.36	-0.24
5 pre	2.04	2.38						0.07	-0.17	0.23			
5 int1	2.01							0.02		0.24			-0.32
5 int2	2.07		2.37	2.53		1.37		0.01		0.19	-0.29	-0.16	-0.31
5 int3	2.06		1.98	2.29	1.98	1.58	1.59	0.17		0.14	-0.34	-0.24	-0.33
5 ts5	2.08		2.24	2.42	1.84	1.39	2.35	-0.12		0.37	-0.29	-0.19	-0.23
5 ts6	2.11		2.29	2.18	2.10	1.44	1.48	0.01		0.09	-0.19	-0.35	-0.24

partial charges on the carbon atoms forming the metal-lacyclobutane core are very consistent and differ to a negligible extent, apart from C3 partial charge, which for **ts5/int5** is 0.1 e higher for 4/5 than for **1**. Larger differences may be observed for the partial charge of the ruthenium atom and carbene carbon atom. For the precatalysts of 4/5 and most of its intermediates and transition states, the partial charges on C_{carbene} are around 0.1 e lower than those for **1**, while the partial charges on Ru are 0.1 e higher than those for **1**. This situation is reversed for the **ts5/int5** pair, where the partial charges on C_{carbene} are around 0.1 e higher than those for **1**, while the partial charges on Ru are 0.1 e lower than those for **1**.

This result can be explained by noticing that the additional negative charge introduced to the carbene in **4** and **5** affects its electronic structure in such a manner that the carbene carbon atom becomes more negatively charged with respect to **1**. Such a change, in turn, affects the ruthenium core to make it slightly more positively charged than for **1**, but overall, the changes are relatively small. Even smaller changes can be observed for the positively charged complexes **2** and **3**, where the partial charge of the carbene carbon atom is virtually identical to the Hoveyda–Grubbs catalyst, and the small discrepancies between **2/3** and **1** can be observed only for the Ru atom. These results reinforce the idea that the influence of the

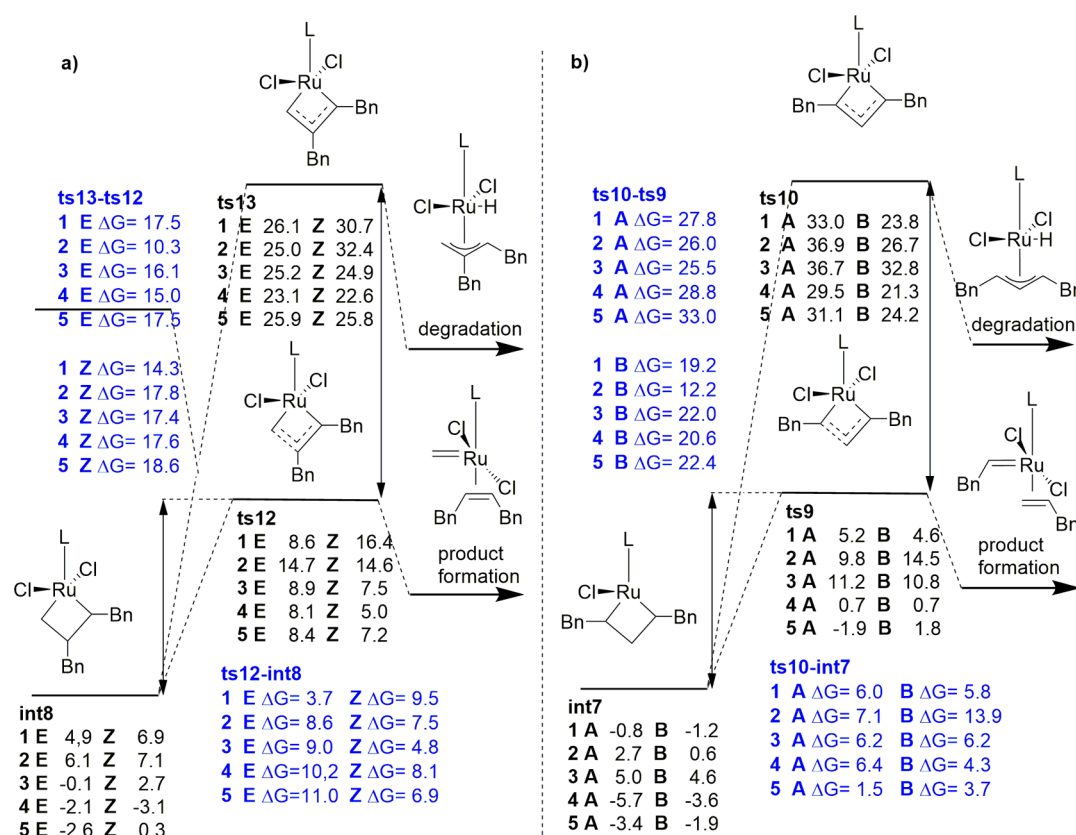


Figure 10. Relative Gibbs free energies profile (kcal/mol, all relative to precatalysts **pre**) for the crucial reactions of the allylbenzene self-metathesis and decomposition of **1–5**.

additional +1 charge on the catalytic properties of Hoveyda–Grubbs catalysts is negligible, while the impact of the additional -1 charge is small, but may lead to substantial differences in catalytic activities.³² In the case of **4/5**, the differences, however, can also be attributed to the lack of the mesityl moieties, which were shown to incorporate the excess negative charge.⁵²

There is one more important Gibbs free energy difference that warrants everyone's attention, namely, the difference between the barrier for ethylene-driven decomposition (**ts6**) and barrier of the self-metathesis of allylbenzene (**ts12**). If these energy barriers are similar or the latter is higher than the former, ethylene may slow down allylbenzene metathesis and the formation of the desired product, 1,4-diphenylbut-2-ene, and make the decomposition of the catalysts as likely as the propagation of metathesis. In the case of allylbenzene self-metathesis, the highest free energy barrier is usually attributed to the transition state of metallacyclobutane disassembly (**ts5/ts12**),^{63,64} while for olefin-driven degradation, the crucial barrier is for transition states **ts6** and **ts13**, leading to van Rensburg's decomposition. Additionally, even though the formation of **int7** leads to unproductive metathesis via **ts9**, it can also potentially lead to catalyst decomposition via **ts10**.

The results presented in **Figure 10** show a few interesting features. First, the differences in Gibbs free energies between **ts12**, the metathesis path (to form the final product), and **ts13**, the van Rensburg's decomposition path for allylbenzene, are quite high (all above 14 kcal/mol apart from **2** with 10 kcal/mol), suggesting that at this point, decomposition does not occur at all. This is consistent with previous results presented here where intermediates with one benzyl moiety were shown

to be more stable than those with just hydrogen atoms (see **Figures 7–9**) and with previous decomposition studies.^{37,40} Second, all the estimates of the Gibbs free energy of **ts12**, which leads to the final product, are lower than the estimates for the ethylene-driven decomposition transition state **ts6** (**Figure 7**). Finally, for some catalysts, there are large differences in the **ts12** energy barriers, leading to the E or Z isomers of the final product, clearly favoring one isomer over the other.

The **int7** intermediate seems to be slightly more stable than **int8**, but as mentioned before, it cannot produce the final product and can only lead to either **int5** or decompose via **ts10**. The decomposition barriers with respect to the precatalyst are quite high (above 26 kcal/mol) for all studied catalysts apart from two isomers of **int7** bearing the negative charge with values of 21–24 kcal/mol. It is worth mentioning, however, that for **4** and **5**, the barriers of unproductive metathesis (**ts9**) are very low with respect to both the precatalyst and intermediate **int7**, resulting in a very high difference between the Gibbs free energies of **ts9** versus **ts10**. As a result, it is likely that the catalyst is, here, trapped in the unproductive metathesis cycle with little or no decomposition occurring at this stage of the entire catalytic cycle.

As explained above, the second known olefin-driven decomposition pathway, suggested by Jensen, has relatively high Gibbs free energy barriers and is unlikely to contribute a lot to the studied catalysts' degradation.⁴⁰ This is, however, not the case for the third and final known olefin-driven decomposition pathway, namely, the bimolecular coupling of methylidene intermediates.^{38,39} To obtain a complete picture of the impact of investigated carbenes on the decomposition

rates of charged metathesis catalysts, we also studied this mechanism. The results (Figure 11) show quite different

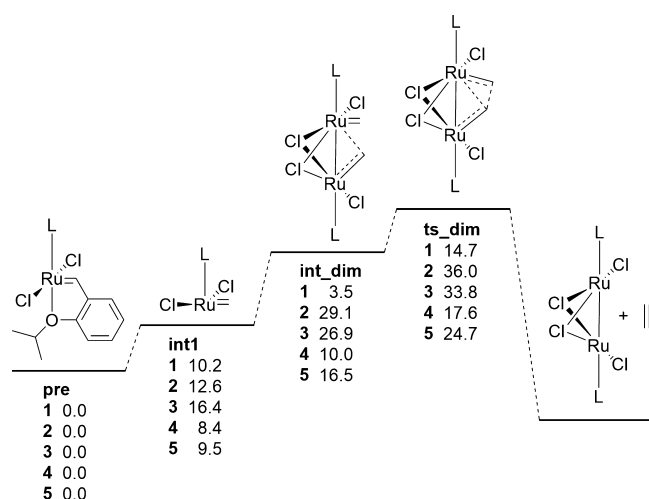


Figure 11. Relative Gibbs free energy profile (kcal/mol, all relative to precatalysts **pre**) for the crucial intermediates and transition states of the diruthenium decomposition pathway of 1–5.

propensity of these catalysts to bimolecular decomposition. The standard Hoveyda–Grubbs catalyst spontaneously forms the diruthenium dimer from methylidene and has a relatively low decomposition barrier using this path, in agreement with former experimental data.³⁹ The results for charged catalysts show that, in general, charged carbenes tend to destabilize the diruthenium intermediates, giving higher relative Gibbs free energies of the dimer with respect to the methylidene monomers. This effect is particularly pronounced for positively charged carbenes, resulting in such high energies of the methylidene dimers, that is, it is unlikely that they are produced at all. It is also a rather expected result because one can argue that two positive charges located that close to ruthenium atoms destabilize dimers because of repulsive electrostatic interactions. For negatively charged carbenes **c4** and **c5**, we can observe a similar effect, but here, the relative energies depend also on the distance of the formal charge to the ruthenium core. Dimer with **c5** carbene with the formal charge next to the imidazole ring has a relatively high Gibbs free energy with respect to its methylidene monomer and a high barrier of decomposition. On the other hand, if the negative formal charge is located further from imidazole, destabilization is much weaker and the Gibbs free energies of transition states, leading to decomposition for dimer bearing the **c4** carbene, is similar to the van Rensburg decomposition pathway.

4. CONCLUSIONS

The stability of ruthenium olefin catalysts is one of their most important features when designing new catalysts, particularly in the context of green chemistry. Despite this fact, it has been reported only for a fraction of ruthenium catalysts and a broad understanding of the relationship between the structure of catalysts and their degradation propensities is missing. In this work, we presented a systematic study of the degradation pathways for Hoveyda–Grubbs catalysts and their model derivatives bearing formal +1 or –1 charge in the carbene part to obtain such structure–activity relationships.

We show that the introduction of the positive charge does not affect the van Rensburg degradation pathway barriers and the entire metathesis catalytic cycle. This is in line with our previous investigation and a number of experimental studies showing that the additional +1 charge on carbene has also little impact on the overall reactivity of ruthenium metathesis catalysts.^{32,51} Considering the bimolecular coupling decomposition pathway, however, the formal positive charge close to the imidazole moiety destabilizes the diruthenium intermediate, making this pathway highly unlikely for positively charged carbenes.

Conversely, the excess negative charge on carbene has a relatively large influence on the entire catalytic system. Although the decomposition transition state barriers (for both the van Rensburg mechanism and bimolecular coupling) for these complexes are very similar to the Hoveyda–Grubbs catalyst, the differences between the decomposition and metathesis transition state barriers are higher than those for cationic and neutral complexes. As a result, anionic Hoveyda–Grubbs-like complexes are predicted to be slightly more stable than the Hoveyda–Grubbs complex and as efficient as standard neutral and cationic catalysts in olefin metathesis. We hope that this result will boost the efforts in synthesizing negatively charged ruthenium metathesis complexes as they may prove a new subfamily of metathesis catalysts with distinct features, potentially useful in preparation of various chemicals.

■ ASSOCIATED CONTENT

Supporting Information

The Supporting Information is available free of charge at <https://pubs.acs.org/doi/10.1021/acs.jpca.0c03096>.

Detailed energies for all studied systems (PDF)

Cartesian coordinates of all studied systems (XYZ)

■ AUTHOR INFORMATION

Corresponding Author

Bartosz Trzaskowski – Centre of New Technologies, University of Warsaw, 02-097 Warszawa, Poland; orcid.org/0000-0003-2385-1476; Email: b.trzaskowski@cent.uw.edu.pl

Authors

Magdalena Jawiczuk – Centre of New Technologies, University of Warsaw, 02-097 Warszawa, Poland

Anna Marczyk – Centre of New Technologies and Faculty of Chemistry, University of Warsaw, 02-097 Warszawa, Poland

Katarzyna Młodzikowska-Pieńko – Centre of New Technologies and Faculty of Chemistry, University of Warsaw, 02-097 Warszawa, Poland

Complete contact information is available at:

<https://pubs.acs.org/doi/10.1021/acs.jpca.0c03096>

Author Contributions

§M.J., A.M., and K.M.-P. contributed equally to the work.

Notes

The authors declare no competing financial interest.

■ ACKNOWLEDGMENTS

We acknowledge research support from the National Science Centre grants UMO-2016/22/E/ST4/00573 and UMO-2016/23/G/ST5/04297.

REFERENCES

- (1) Arduengo, A. J.; Harlow, R. L.; Kline, M. A. Stable Crystalline Carbene. *J. Am. Chem. Soc.* **1991**, *113*, 361–363.
- (2) Enders, D.; Niemeier, O.; Henseler, A. Organocatalysis by N-Heterocyclic Carbenes. *Chem. Rev.* **2007**, *107*, 5606–5655.
- (3) Vougioukalakis, G. C.; Grubbs, R. H. Ruthenium-Based Heterocyclic Carbene-Coordinated Olefin Metathesis Catalysts. *Chem. Rev.* **2010**, *110*, 1746–1787.
- (4) Garber, S. B.; Kingsbury, J. S.; Gray, B. L.; Hoveyda, A. H. Efficient and Recyclable Monomeric and Dendritic Ru-Based Metathesis Catalysts. *J. Am. Chem. Soc.* **2000**, *122*, 8168–8179.
- (5) Dröge, T.; Glorius, F. The Measure of All Rings—N-Heterocyclic Carbenes. *Angew. Chem., Int. Ed.* **2010**, *49*, 6940–6952.
- (6) Comas-Vives, A.; Harvey, J. N. How Important Is Backbonding in Metal Complexes Containing N-Heterocyclic Carbenes? Structural and NBO Analysis. *Eur. J. Inorg. Chem.* **2011**, 5025–5035.
- (7) Majhi, P. K.; Schnakenburg, G.; Kelemen, Z.; Nyulaszi, L.; Gates, D. P.; Streubel, R. Synthesis of an Imidazolium Phosphanide Zwitterion and Its Conversion into Anionic Imidazol-2-ylidene Derivatives. *Angew. Chem., Int. Ed.* **2013**, *52*, 10080–10083.
- (8) Benhamou, L.; César, V.; Gornitzka, H.; Lugan, N.; Lavigne, G. Imidazole-2-ylidene-4-Olate: An Anionic N-Heterocyclic Carbene Pre-Programmed for Further Derivatization. *Chem. Commun.* **2009**, 4720–4722.
- (9) Biju, A. T.; Hirano, K.; Fröhlich, R.; Glorius, F. Switching the Electron-Donor Properties of N-Heterocyclic Carbenes by a Facile Deprotonation Strategy. *Chem.—Asian J.* **2008**, *4*, 1786–1789.
- (10) Danopoulos, A. A.; Monakhov, K. Y.; Braunstein, P. Anionic N-Heterocyclic Carbene Ligands from Mesoionic Imidazolium Precursors: Remote Backbone Arylimino Substitution Directs Carbene Coordination. *Chem.—Eur. J.* **2013**, *19*, 450–455.
- (11) César, V.; Mallardo, V.; Nano, A.; Dahm, G.; Lugan, N.; Lavigne, G.; Bellemin-Laponnaz, S. IMes-Acac: Hybrid Combination of Diaminocarbene and Acetylacetonato Sub-Units into a New Anionic Ambidentate NHC Ligand. *Chem. Commun.* **2015**, *51*, 5271–5274.
- (12) Gupta, V.; Karthik, V.; Anantharaman, G. Labile Dioxo-Functionalised Zwitterionic Imidazolium Salt: Access to Zwitterionic and Neutral Imidazolidin-2-ylidene Derivatives and π -Acceptor Properties of Imidazolidine-2-Selones. *RSC Adv.* **2015**, *5*, 87888–87896.
- (13) Kronig, S.; Theuergarten, E.; Daniliuc, C. G.; Jones, P. G.; Tamm, M. Anionic N-Heterocyclic Carbenes That Contain a Weakly Coordinating Borate Moiety. *Angew. Chem.* **2012**, *124*, 3294–3298.
- (14) Wacker, A.; Yan, C. G.; Kaltenpoth, G.; Ginsberg, A.; Arif, A. M.; Ernst, R. D.; Pritzkow, H.; Siebert, W. Metal Complexes of Anionic 3-Borane-1-Alkylimidazol-2-ylidene Derivatives. *J. Organomet. Chem.* **2002**, *641*, 195–202.
- (15) Mungur, S. A.; Liddle, S. T.; Wilson, C.; Sarsfield, M. J.; Arnold, P. L. Bent Metal Carbene Geometries in Amido N-Heterocyclic Carbene Complexes. *Chem. Commun.* **2004**, 2738–2739.
- (16) Danopoulos, A. A.; Braunstein, P. ‘Janus-Type’ Organopotassium Chemistry Observed in Deprotonation of Mesoionic Imidazolium Aminides and Amino N-Heterocyclic Carbenes: Coordination and Organometallic Polymers. *Chem. Commun.* **2014**, *50*, 3055–3057.
- (17) Nasr, A.; Winkler, A.; Tamm, M. Anionic N-Heterocyclic Carbenes: Synthesis, Coordination Chemistry and Applications in Homogeneous Catalysis. *Coord. Chem. Rev.* **2016**, *316*, 68–124.
- (18) Grudziń, K.; Trzaskowski, B.; Smoleń, M.; Gajda, R.; Woźniak, K.; Grela, K. Hoveyda–Grubbs Catalyst Analogues Bearing the Derivatives of N-Phenylpyrrol in the Carbene Ligand – Structure, Stability, Activity and Unique Ruthenium–Phenyl Interactions. *Dalton Trans.* **2017**, *46*, 11790–11799.
- (19) Pazio, A.; Woźniak, K.; Grela, K.; Trzaskowski, B. Nitrenium Ions and Trivalent Boron Ligands as Analogues of N-Heterocyclic Carbenes in Olefin Metathesis: A Computational Study. *Dalton Trans.* **2015**, *44*, 20021–20026.
- (20) Hildebrandt, B.; Frank, W.; Ganter, C. A Cationic N-Heterocyclic Carbene with an Organometallic Backbone: Synthesis and Reactivity. *Organometallics* **2011**, *30*, 3483–3486.
- (21) Schwedtmann, K.; Schoemaker, R.; Hennersdorf, F.; Bauzá, A.; Frontera, A.; Weiss, R.; Weigand, J. J. Cationic 5-Phosphonio-Substituted N-Heterocyclic Carbenes. *Dalton Trans.* **2016**, *45*, 11384–11396.
- (22) Ruamps, M.; Lugan, N.; César, V. A Cationic N-Heterocyclic Carbene Containing an Ammonium Moiety. *Organometallics* **2017**, *36*, 1049–1055.
- (23) Valdés, H.; Poyatos, M.; Peris, E. A Pyrene-Based N-Heterocyclic Carbene: Study of Its Coordination Chemistry and Stereoelectronic Properties. *Organometallics* **2014**, *33*, 394–401.
- (24) Verlinden, K.; Ganter, C. Converting a Perimidine Derivative to a Cationic N-Heterocyclic Carbene. *J. Organomet. Chem.* **2014**, *750*, 23–29.
- (25) Hildebrandt, B.; Raub, S.; Frank, W.; Ganter, C. Expanding the Chemistry of Cationic N-Heterocyclic Carbenes: Alternative Synthesis, Reactivity, and Coordination Chemistry. *Chem.—Eur. J.* **2012**, *18*, 6670–6678.
- (26) Jordan, J. P.; Grubbs, R. H. Small-Molecule N-Heterocyclic Carbene-Containing Olefin-Metathesis Catalysts for Use in Water. *Angew. Chem., Int. Ed.* **2007**, *46*, 5152–5155.
- (27) Iglesias-Sigüenza, J.; Izquierdo, C.; Díez, E.; Fernández, R.; Lassaletta, J. M. N-Heterocyclic Cationic Carbene Ligands. Synthesis, Reactivity and Coordination Chemistry. *Dalton Trans.* **2018**, *47*, 5196–5206.
- (28) Skowerski, K.; Szczepaniak, G.; Wierzbicka, C.; Gulajski, Ł.; Bieniek, M.; Grela, K. Highly Active Catalysts for Olefin Metathesis in Water. *Catal. Sci. Technol.* **2012**, *2*, 2424–2427.
- (29) Skowerski, K.; Wierzbicka, C.; Szczepaniak, G.; Gulajski, Ł.; Bieniek, M.; Grela, K. Easily Removable Olefin Metathesis Catalysts. *Green Chem.* **2012**, *14*, 3264–3268.
- (30) Balof, S. L.; P’Pool, S. J.; Berger, N. J.; Valente, E. J.; Shiller, A. M.; Schanz, H.-J. Olefin Metathesis Catalysts Bearing a PH-Responsive NHC Ligand: A Feasible Approach to Catalyst Separation from RCM Products. *Dalton Trans.* **2008**, 5791–5799.
- (31) Kośnik, W.; Grela, K. Synthesis of Functionalised N-Heterocyclic Carbene Ligands Bearing a Long Spacer and Their Use in Olefin Metathesis. *Dalton Trans.* **2013**, *42*, 7463–7467.
- (32) Jawiczuk, M.; Janaszkiwicz, A.; Trzaskowski, B. The Influence of the Cationic Carbenes on the Initiation Kinetics of Ruthenium-Based Metathesis Catalysts; a DFT Study. *Beilstein J. Org. Chem.* **2018**, *14*, 2872–2880.
- (33) Malecki, P.; Gajda, K.; Gajda, R.; Woźniak, K.; Trzaskowski, B.; Kajetanowicz, A.; Grela, K. Specialized Ruthenium Olefin Metathesis Catalysts Bearing Bulky Unsymmetrical NHC Ligands: Computations, Synthesis, and Application. *ACS Catal.* **2019**, *9*, 587–598.
- (34) César, V.; Zhang, Y.; Kośnik, W.; Zieliński, A.; Rajkiewicz, A. A.; Ruamps, M.; Bastin, S.; Lugan, N.; Lavigne, G.; Grela, K. Ruthenium Catalysts Supported by Amino-Substituted N-Heterocyclic Carbene Ligands for Olefin Metathesis of Challenging Substrates. *Chem.—Eur. J.* **2017**, *23*, 1950–1955.
- (35) Hong, S. H.; Day, M. W.; Grubbs, R. H. Decomposition of a Key Intermediate in Ruthenium-Catalyzed Olefin Metathesis Reactions. *J. Am. Chem. Soc.* **2004**, *126*, 7414–7415.
- (36) Hong, S. H.; Wenzel, A. G.; Salguero, T. T.; Day, M. W.; Grubbs, R. H. Decomposition of Ruthenium Olefin Metathesis Catalysts. *J. Am. Chem. Soc.* **2007**, *129*, 7961–7968.
- (37) van Rensburg, W. J.; Steynberg, P. J.; Kirk, M. M.; Meyer, W. H.; Forman, G. S. Mechanistic Comparison of Ruthenium Olefin Metathesis Catalysts: DFT Insight into Relative Reactivity and Decomposition Behavior. *J. Organomet. Chem.* **2006**, *691*, 5312–5325.
- (38) Bailey, G. A.; Foscatto, M.; Higman, C. S.; Day, C. S.; Jensen, V. R.; Fogg, D. E. Bimolecular Coupling as a Vector for Decomposition of Fast-Initiating Olefin Metathesis Catalysts. *J. Am. Chem. Soc.* **2018**, *140*, 6931–6944.

- (39) Nascimento, D. L.; Fogg, D. E. Origin of the Breakthrough Productivity of Ruthenium–Cyclic Alkyl Amino Carbene Catalysts in Olefin Metathesis. *J. Am. Chem. Soc.* **2019**, *141*, 19236–19240.
- (40) Engel, J.; Smit, W.; Foscatto, M.; Occhipinti, G.; Törnroos, K. W.; Jensen, V. R. Loss and Reformation of Ruthenium Alkylidene: Connecting Olefin Metathesis, Catalyst Deactivation, Regeneration, and Isomerization. *J. Am. Chem. Soc.* **2017**, *139*, 16609–16619.
- (41) Galan, B. R.; Gembicky, M.; Dominiak, P. M.; Keister, J. B.; Diver, S. T. Carbon Monoxide-Promoted Carbene Insertion into the Aryl Substituent of an N-Heterocyclic Carbene Ligand: Buchner Reaction in a Ruthenium Carbene Complex. *J. Am. Chem. Soc.* **2005**, *127*, 15702–15703.
- (42) Galan, B. R.; Kalbarczyk, K. P.; Szczepankiewicz, S.; Keister, J. B.; Diver, S. T. A Rapid and Simple Cleanup Procedure for Metathesis Reactions. *Org. Lett.* **2007**, *9*, 1203–1206.
- (43) Galan, B. R.; Pitak, M.; Gembicky, M.; Keister, J. B.; Diver, S. T. Ligand-Promoted Carbene Insertion into the Aryl Substituent of an N-Heterocyclic Carbene Ligand in Ruthenium-Based Metathesis Catalysts. *J. Am. Chem. Soc.* **2009**, *131*, 6822–6832.
- (44) Szczepaniak, G.; Ruszczynska, A.; Kosiński, K.; Bulska, E.; Grela, K. Highly Efficient and Time Economical Purification of Olefin Metathesis Products from Metal Residues Using an Isocyanide Scavenger. *Green Chem.* **2018**, *20*, 1280–1289.
- (45) Poater, A.; Ragone, F.; Correa, A.; Cavallo, L. Exploring the Reactivity of Ru-Based Metathesis Catalysts with a π -Acid Ligand Trans to the Ru–Ylidene Bond. *J. Am. Chem. Soc.* **2009**, *131*, 9000–9006.
- (46) Beach, N. J.; Camm, K. D.; Fogg, D. E. Hydrogenolysis versus Methanolysis of First- and Second-Generation Grubbs Catalysts: Rates, Speciation, and Implications for Tandem Catalysis. *Organometallics* **2010**, *29*, 5450–5455.
- (47) Manzini, S.; Poater, A.; Nelson, D. J.; Cavallo, L.; Slawin, A. M. Z.; Nolan, S. P. Insights into the Decomposition of Olefin Metathesis Precatalysts. *Angew. Chem., Int. Ed.* **2014**, *53*, 8995–8999.
- (48) Ireland, B. J.; Dobigny, B. T.; Fogg, D. E. Decomposition of a Phosphine-Free Metathesis Catalyst by Amines and Other Bronsted Bases: Metallacyclobutane Deprotonation as a Major Deactivation Pathway. *ACS Catal.* **2015**, *5*, 4690–4698.
- (49) Jawiczuk, M.; Młodzikowska-Pieńko, K.; Osella, S.; Trzaskowski, B. Molecular Modeling of Mechanisms of Decomposition of Ruthenium Metathesis Catalysts by Acrylonitrile. *Organometallics* **2020**, *39*, 239–246.
- (50) Rouen, M.; Queval, P.; Borré, E.; Falivene, L.; Poater, A.; Berthod, M.; Hugues, F.; Cavallo, L.; Baslé, O.; Olivier-Bourbigou, H.; Mauduit, M. Selective Metathesis of α -Olefins from Bio-Sourced Fischer–Tropsch Feeds. *ACS Catal.* **2016**, *6*, 7970–7976.
- (51) Jana, A.; Grela, K. Forged and Fashioned for Faithfulness—Ruthenium Olefin Metathesis Catalysts Bearing Ammonium Tags. *Chem. Commun.* **2018**, *54*, 122–139.
- (52) Młodzikowska, K.; Rajkiewicz, A. A.; Grela, K.; Trzaskowski, B. Boron–Boron, Carbon–Carbon and Nitrogen–Nitrogen Bonding in N-Heterocyclic Carbenes and Their Diazaboryl and Triazole Analogues: Wanzlick Equilibrium Revisited. *New J. Chem.* **2018**, *42*, 6183–6190.
- (53) Jolly, P. I.; Marczyk, A.; Małecki, P.; Ablialimov, O.; Trzybiński, D.; Woźniak, K.; Osella, S.; Trzaskowski, B.; Grela, K. Azoliniums, Adducts, NHCs and Azomethine Ylides: Divergence in Wanzlick Equilibrium and Olefin Metathesis Catalyst Formation. *Chem.—Eur. J.* **2018**, *24*, 4785–4789.
- (54) Smoleń, M.; Marczyk, A.; Kośnik, W.; Trzaskowski, B.; Kajetanowicz, A.; Grela, K. Ruthenium-Catalysed Olefin Metathesis in Environmentally Friendly Solvents: 2-Methyltetrahydrofuran Revisited. *Eur. J. Org. Chem.* **2019**, 640–646.
- (55) Gawin, R.; Tracz, A.; Chwalba, M.; Kozakiewicz, A.; Trzaskowski, B.; Skowerski, K. Cyclic Alkyl Amino Ruthenium Complexes—Efficient Catalysts for Macrocyclization and Acrylonitrile Cross Metathesis. *ACS Catal.* **2017**, *7*, 5443–5449.
- (56) Rajkiewicz, A. A.; Skowerski, K.; Trzaskowski, B.; Kajetanowicz, A.; Grela, K. 2-Methyltetrahydrofuran as a Solvent of Choice for Spontaneous Metathesis/Isomerization Sequence. *ACS Omega* **2019**, *4*, 1831–1837.
- (57) Barbasiewicz, M.; Bieniek, M.; Michrowska, A.; Szadkowska, A.; Makal, A.; Woźniak, K.; Grela, K. Probing of the Ligand Anatomy: Effects of the Chelating Alkoxy Ligand Modifications on the Structure and Catalytic Activity of Ruthenium Carbene Complexes. *Adv. Synth. Catal.* **2007**, *349*, 193–203.
- (58) LaJohn, L. A.; Christiansen, P. A.; Ross, R. B.; Atashroo, T.; Ermler, W. C. Ab Initio Relativistic Effective Potentials with Spin–Orbit Operators. III. Rb through Xe. *J. Chem. Phys.* **1987**, *87*, 2812–2824.
- (59) Bochevarov, A. D.; Harder, E.; Hughes, T. F.; Greenwood, J. R.; Braden, D. A.; Philipp, D. M.; Rinaldo, D.; Halls, M. D.; Zhang, J.; Friesner, R. A. Jaguar: A High-Performance Quantum Chemistry Software Program with Strengths in Life and Materials Sciences. *Int. J. Quantum Chem.* **2013**, *113*, 2110–2142.
- (60) Ashworth, I. W.; Hillier, I. H.; Nelson, D. J.; Percy, J. M.; Vincent, M. A. What Is the Initiation Step of the Grubbs–Hoveyda Olefin Metathesis Catalyst? *Chem. Commun.* **2011**, *47*, 5428–5430.
- (61) Thiel, V.; Hendann, M.; Wannowius, K.-J.; Plenio, H. On the Mechanism of the Initiation Reaction in Grubbs–Hoveyda Complexes. *J. Am. Chem. Soc.* **2012**, *134*, 1104–1114.
- (62) Janse van Rensburg, W.; Steynberg, P. J.; Meyer, W. H.; Kirk, M. M.; Forman, G. S. DFT Prediction and Experimental Observation of Substrate-Induced Catalyst Decomposition in Ruthenium-Catalyzed Olefin Metathesis. *J. Am. Chem. Soc.* **2004**, *126*, 14332–14333.
- (63) Fomine, S.; Tlenkopatchev, M. A. Ring-Opening of Cyclohexene via Metathesis by Ruthenium Carbene Complexes. A Computational Study. *Organometallics* **2007**, *26*, 4491–4497.
- (64) Śliwa, P.; Kurleto, K.; Handzlik, J.; Rogalski, S.; Żak, P.; Wyrzykiewicz, B.; Pietraszuk, C. Regioselectivity of Stoichiometric Metathesis of Vinylsilanes with Second-Generation Grubbs Catalyst: A Combined DFT and Experimental Study. *Organometallics* **2016**, *35*, 621–628.